

Lattice-Induced Double-Valley Degeneracy Lifting in Graphene by a Magnetic Field

Igor A. Luk'yanchuk^{1,2} and Alexander M. Bratkovsky³

¹University of Picardie Jules Verne, Laboratory of Condensed Matter Physics, Amiens, 80039, France

²L. D. Landau Institute for Theoretical Physics, Moscow, Russia

³Hewlett-Packard Laboratories, 1501 Page Mill Road, Palo Alto, California 94304

(Dated: February 6, 2020)

We show that the recently discovered double-valley splitting of the low-lying Landau level(s) in the Quantum Hall Effect in graphene can be explained as *perturbative* orbital interaction of intra- and inter-valley microscopic orbital currents with a magnetic field. This effect is provided by the translational-non-invariant terms corresponding to graphene's crystallographic honeycomb symmetry but do not exist in the relativistic theory of massless Dirac Fermions in Quantum Electrodynamics. We discuss recent data in view of these results.

PACS numbers: 71.70.-d, 73.43.-f, 81.05.Uw

The recent discovery of massless charge carriers with linear conic spectrum - Dirac fermions (DF) in both graphite [1] and graphene [2, 3] has prompted researchers to revisit many basic ideas in Solid State Physics based on relativistic particle physics on a lattice. The existence of Dirac fermions has been confirmed by direct ARPES [4, 5] and STS [6] measurements and by Quantum Hall Effect (QHE) measurements in both graphite [7, 8] and graphene [2, 3]. It has been recognized that the analogy between DF in graphene and relativistic massless DF in Quantum Electrodynamics (QED) can be used fruitfully to explore the properties of graphene-based systems [9]. One of the most important consequences of this analogy is the peculiar quantization of relativistic Landau Levels (LLs) in a magnetic field that are symmetric for positive (electron) and negative (hole) energies. The LL energies are proportional $\pm\sqrt{n}$ as a function of the level number n away from the zero LL ($n = 0$) that is positioned exactly at the Dirac point where electron and hole spectra touch at zero magnetic field, $\mathbf{H} = 0$. In addition to the infinite Landau degeneracy, each level is double spin-degenerate, which is a direct consequence of the relativistic (Lorentz) invariance of the QED equations.

The QED double-spin degeneracy corresponds to the double-valley degeneracy of LLs in graphene and, together with conventional spin-degeneracy (not considered by the QED analogy), produces the conductance steps of $4e^2/h$ [10] observed in the semi-integer QHE [2, 3], double the size of standard steps. Importantly, therefore, the recently discovered double-valley splitting for (at least) the zero Landau level [11, 12] indicates a breakdown of relativistic invariance in graphene. Several mechanisms [13] based on *spontaneous* symmetry breaking driven by either long-range Coulomb interaction [14, 15, 16, 17, 18], field-enhanced electron-phonon interaction [19], disorder [20, 21, 22] or edge effects [12, 23, 24] have been proposed to explain this phenomenon.

In this paper, we demonstrate that the valley gap opening for low-lying LLs is the *intrinsic* property of graphene-like systems. These systems have a honey-

comb crystallographic group that is different from the relativistic Lorentz group in QED albeit resulting in a similar Dirac-like equation for non-interacting fermions in zero magnetic field, $\mathbf{H} = 0$. The difference becomes apparent in an applied magnetic field when the additional translational-non-invariant terms accounting for interaction of microscopic intra- and inter-valley orbital currents with the magnetic field appear in the graphene Hamiltonian. The effect of the double-valley LL splitting has, therefore, a much more natural explanation as a *perturbative* non-critical orbital splitting that is of the same order as the standard Zeeman spin-splitting.

We first consider the origin and symmetry properties of the Hamiltonian, the spectrum, and the wave functions of conducting electrons (holes) in the vicinity of two crystallographically nonequivalent opposite corners $\mathbf{K}_{1,2}$ (also denoted as \mathbf{K} and \mathbf{K}') of the hexagonal Brillouin Zone of graphene *at zero field*, $\mathbf{H} = 0$. The wave functions of the zero-energy states are located exactly at $\mathbf{K}_{1,2}$ and can be linearly expanded over a 4-component Bloch basis (irreducible representation) of the K-point [25]:

$$\tilde{\Psi} \equiv \{\Psi_i\}_{i=1-4} = \{\Psi_{K_1}^A, \Psi_{K_1}^B, \Psi_{K_2}^B, \Psi_{K_2}^A\}^T. \quad (1)$$

(for symmetry reasons our set $\{\Psi_i\}$ is different from the commonly used $\{\Psi_{K_1}^A, \Psi_{K_1}^B, \Psi_{K_2}^A, \Psi_{K_2}^B\}$).

It is the transformation properties of spinor-like function $\tilde{\Psi}$ under the action of the graphene crystallographic

TABLE I: Transformation properties of the Bloch spinor $\tilde{\Psi}$ ($\varepsilon = e^{2\pi i/3}$)

	C_6	σ_x	σ_y	\hat{T}_{12}
$\Psi_{K_1}^A$	$\bar{\varepsilon}\Psi_{K_2}^B$	$\Psi_{K_2}^A$	$\Psi_{K_1}^B$	$\varepsilon\Psi_{K_1}^A$
$\Psi_{K_1}^B$	$\varepsilon\Psi_{K_2}^A$	$\Psi_{K_2}^B$	$\Psi_{K_1}^A$	$\varepsilon\Psi_{K_1}^B$
$\Psi_{K_2}^A$	$\varepsilon\Psi_{K_1}^B$	$\Psi_{K_1}^A$	$\Psi_{K_2}^B$	$\bar{\varepsilon}\Psi_{K_2}^A$
$\Psi_{K_2}^B$	$\bar{\varepsilon}\Psi_{K_1}^A$	$\Psi_{K_1}^B$	$\Psi_{K_2}^A$	$\bar{\varepsilon}\Psi_{K_2}^B$

group

$$G = \{C_6, C_3, C_2, \sigma_x, \sigma_y, R\} \times \{\mathbf{T}_1, \mathbf{T}_2\}, \quad (2)$$

(Table I) that define all the physical properties of charge carriers in graphene. Here, $\mathbf{T}_{1,2}$ are the lattice translations; other notation are the same as in [25]. The physical properties can be obtained either directly from the standard Tables of Irreducible Representations of Crystallographic Groups [26] or from the explicit form of $\tilde{\Psi}$ in a tight-binding approximation of the carbon p_z orbitals marked as $\pi(\mathbf{r})$ (see also Fig. 1):

$$\Psi_{K_{1,2}}^{A(B)} = e^{\frac{2}{3}s_{A(B)}i\pi} \sum_{nm} e^{s_{K_{1,2}}\frac{2}{3}i\pi(n+m)} \pi(\mathbf{r} - \mathbf{t}_{nm}^{A(B)}) \quad (3)$$

where $s_{A(B)} = +(-)1$, $s_{K_{1,2}} = \pm 1$ and $\mathbf{t}_{nm}^{A(B)}$ are the A (B) sublattice coordinates.

Wave functions of states deviating from $\mathbf{K}_{1,2}$ by a small vector $\mathbf{k} = (k_x, k_y)$ can also be expanded over the basis $\Psi_i(\mathbf{r})$, but with slowly space-varying envelopes $\tilde{F}^{\mathbf{k}} \equiv F_i^{\mathbf{k}}(\mathbf{r})$:

$$\Phi^{\mathbf{k}}(\mathbf{r}) = \sum_{i=1}^4 F_i^{\mathbf{k}}(\mathbf{r}) \Psi_i(\mathbf{r}). \quad (4)$$

The energy spectrum $E(\mathbf{k})$ and the corresponding envelope functions $\tilde{F}^{\mathbf{k}}(\mathbf{r})$ are the eigenvalues and eigenfunctions of the usual $\mathbf{K}\mathbf{k}$ -perturbation equation:

$$\hat{H} \tilde{F}^{\mathbf{k}}(\mathbf{r}) = E(\mathbf{k}) \tilde{F}^{\mathbf{k}}(\mathbf{r}) \quad (5)$$

where the $\mathbf{K}\mathbf{k}$ -perturbation Hamiltonian,

$$\hat{H} = v \begin{pmatrix} 0 & \hat{k}_x + i\hat{k}_y & 0 & 0 \\ \hat{k}_x - i\hat{k}_y & 0 & 0 & 0 \\ 0 & 0 & 0 & \hat{k}_x + i\hat{k}_y \\ 0 & 0 & \hat{k}_x - i\hat{k}_y & 0 \end{pmatrix} \quad (6)$$

(with $\hat{\mathbf{k}} = -i\hbar\nabla$) was obtained as a most general 4×4 matrix that is linear in \mathbf{k} and conserves the form $\langle \tilde{\Psi} \hat{H} \tilde{\Psi} \rangle$ under the action of the group G .

The Hamiltonian (6) has the structure of the relativistic Dirac Hamiltonian for massless fermions with a linear conical spectrum (Fig. 2a):

$$E(\mathbf{k}) = \pm v|\mathbf{k}|, \quad (7)$$

and the corresponding system of eigenfunctions $\tilde{F}^{\mathbf{k}}(\mathbf{r})$ that is a linear superposition (with arbitrary complex constants c_1, c_2) of two-valley plane-wave functions:

$$\tilde{F}^{\mathbf{k}}(\mathbf{r}) = c_1 \{\pm 1, e^{i\theta}, 0, 0\} e^{i\mathbf{k}\mathbf{r}} + c_2 \{0, 0, \pm 1, e^{i\theta}\} e^{i\mathbf{k}\mathbf{r}}, \quad (8)$$

where $\theta = \arctan(k_x/k_y)$ and the \pm sign corresponds to the upper (lower) branch of the conical spectrum (7).

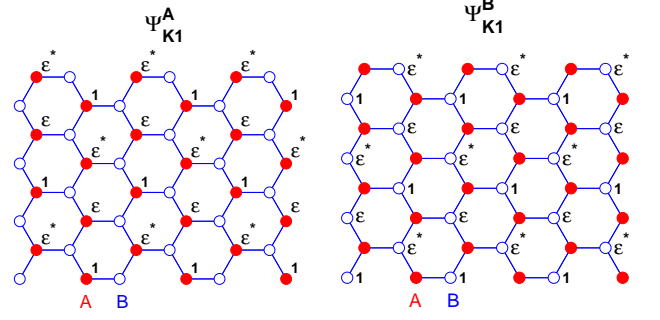


FIG. 1: K_1 -point Bloch functions $\Psi_{K_1}^A$ and $\Psi_{K_1}^B$. The corresponding K_2 -point Bloch functions $\Psi_{K_2}^A$ and $\Psi_{K_2}^B$ are obtained from them by applying complex conjugation.

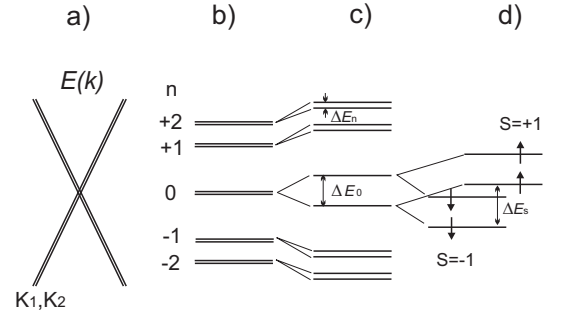


FIG. 2: (a) Two-valley degenerate Dirac-like spectrum $E(k)$ of charge carriers in zero magnetic field, $H = 0$. (b) Landau Level (LL) quantization of Dirac Fermions. (c) Orbital valley splitting of LLs. (d) Additional Zeeman spin-splitting of LLs (only the $n = 0$ level is shown.)

Note, however, that the similarity exploited above with DF in QED is valid only in the vicinity of points $\mathbf{K}_{1,2}$ and is only approximate. In reality, the transformation properties of Ψ_K with respect to the graphene crystallographic group G (Table I) are quite different from those of the real DF transforming with respect to the Lorentz group. This provides the additional contributions to QED-like terms, such as the triangular-wrapped nonlinear kinetic [27] and relativistic-noninvariant Coulomb interaction terms [17].

The Bloch expansion (4) also remains valid in a magnetic field \mathbf{H} , although the slowly varying coefficients $\tilde{F}(\mathbf{r})$ are now classified according to the discrete set of LLs (instead of continuous \mathbf{k}). The usual way of introducing $\mathbf{H} = \nabla \times \mathbf{A}$ consists of the Peierls substitution

$$\hat{\mathbf{k}} \rightarrow \hat{\mathbf{k}} + \frac{|e|\hbar}{c} \mathbf{A}, \quad (9)$$

which in the case of the Hamiltonian (6) is the same as replacing $\hat{k}_x \pm i\hat{k}_y$ by the LL creation (annihilation) operators a^\pm .

The Hamiltonian has a set of discrete LLs having a square-root energy dependence on the level number $n =$

$0, \pm 1, \pm 2, \dots$ in a magnetic field (Fig 2b):

$$E_n = s_{eh} \sqrt{2v^2 |e| \hbar H_z |n| / c}, \quad s_{eh} = \text{sign}(n), \quad (10)$$

which is quite different from the case of massive particles with $E_n = \hbar \omega_c (n + \frac{1}{2}) \geq 0$, ($n = 0, 1, 2, \dots$), and has solutions with values both above and below the zero-energy LL, $E_0 = 0$. The corresponding eigenfunctions can be written as an expansion over the n -th LL eigenfunctions $f_n(r)$:

$$\begin{aligned} \tilde{F}^n(r) = & \{c_1 f_{|n|}(r), s_{eh} i c_1 f_{|n|-1}(r), \\ & c_2 f_{|n|}(r), s_{eh} i c_2 f_{|n|-1}(r)\}, \end{aligned} \quad (11)$$

[note that $f_{-1}(r) \equiv 0$]. Each level, including $n = 0$, has the two-valley degeneracy provided by the complex constants c_1, c_2 , the two-fold spin degeneracy and the infinite Landau degeneracy.

Although the Peierls substitution (9) conserves a relativistic invariance of the Dirac equation in a magnetic field, the discrete crystal lattice background leads to another, *weaker*, requirement that the Hamiltonian of the system should be invariant with respect to the crystallographic group of graphene in a magnetic field:

$$G_H = \{C_6 R, C_3, C_2 R, \sigma_x R, \sigma_y R\}. \quad (12)$$

In particular, this time non-invariant group $G_H \subset G$ does not contain the translations $\mathbf{T}_{1,2}$ that are incompatible with the translational magnetic group. The principal idea of the present work is that the graphene Hamiltonian for charge carriers in magnetic field should have the more general form:

$$\hat{H} = \begin{pmatrix} \lambda \mu_B H_z & v a^+ & \gamma \mu_B H_z & 0 \\ v a^- & -\lambda \mu_B H_z & 0 & -\gamma \mu_B H_z \\ \gamma \mu_B H_z & 0 & \lambda \mu_B H_z & v a^+ \\ 0 & -\gamma \mu_B H_z & v a^- & -\lambda \mu_B H_z \end{pmatrix}, \quad (13)$$

($\mu_B = |e| \hbar / 2mc$) that, besides the Peierls terms a^\pm , contains the “non-relativistic” λ - and γ - corrections provided by the orbital interaction of Bloch electrons with the magnetic field.

These terms keep $\langle \tilde{\Psi} \hat{H} \tilde{\Psi} \rangle$ invariant under the operation of group G_H and are produced by the matrix elements:

$$\begin{aligned} \langle \Psi_{K_1}^A \hat{V} \bar{\Psi}_{K_2}^B \rangle &= - \langle \Psi_{K_1}^B \hat{V} \bar{\Psi}_{K_2}^A \rangle \\ &= \langle \Psi_{K_2}^B \hat{V} \bar{\Psi}_{K_1}^A \rangle = - \langle \Psi_{K_2}^A \hat{V} \bar{\Psi}_{K_1}^B \rangle = \gamma \mu_B H_z, \end{aligned} \quad (14)$$

and

$$\begin{aligned} \langle \Psi_{K_1}^A \hat{V} \bar{\Psi}_{K_1}^A \rangle &= - \langle \Psi_{K_1}^B \hat{V} \bar{\Psi}_{K_1}^B \rangle \\ &= \langle \Psi_{K_2}^B \hat{V} \bar{\Psi}_{K_2}^B \rangle = - \langle \Psi_{K_2}^A \hat{V} \bar{\Psi}_{K_2}^A \rangle = \lambda \mu_B H_z, \end{aligned} \quad (15)$$

of the perturbation operator

$$\hat{V} = -\mathbf{H} \cdot \mathbf{M} = -\frac{e}{2mc} \mathbf{H} \cdot [\mathbf{r} \times \mathbf{p}], \quad (16)$$

where m is the bare electron mass that accounts for the translational-invariant symmetry breakdown due to the discrete crystal background [28, 29]. (Analogous terms for the time-symmetry-breaking field have been proposed in [30] for the orbital part of intrinsic spin-orbit coupling in graphene, which is minute.)

The numerical parameter γ of the matrix elements (14) is estimated in the tight-binding nearest neighbor approximation (between sites A and B) as:

$$\gamma \approx \frac{t/2}{\hbar^2 / m a^2} = 0.4, \quad (17)$$

where $t = 3.033$ eV is the π - π hopping integral, and $a = 1.42 \text{ \AA}$ is the hexagon side (C-C interatomic distance). It is more difficult to estimate the next nearest neighbor parameter λ (between A and A') in (15), since the hopping integral falls off fairly slowly [$t_{\pi\pi}(d) \propto 1/d^2$] but, clearly, $\lambda < \gamma$.

Diagonalization of the Hamiltonian (13) can be easily done in terms of LL wave functions $f_n(r)$, presenting the resulting 4-component eigenfunctions $\tilde{F}^n(r)$ in the form (11) with slightly different coefficients. This again gives the set of discrete LLs with $n = 0, \pm 1, \pm 2, \dots$, having the energies:

$$E_n = s_{eh} \sqrt{2v^2 |e| \hbar H_z |n| / c + (\gamma \pm \lambda)^2 \mu_B^2 H_z^2}. \quad (18)$$

Special attention should be paid to zero LL $n = 0$ with

$$E_0 = (-\lambda \pm \gamma) \mu_B H_z, \quad (19)$$

and

$$\tilde{F}_\pm^n(r) = \{f_0(r), 0, \pm f_0(r), 0\}. \quad (20)$$

The new effect here, illustrated by Fig. 2c, is the valley-splitting of each LL, marked by the \pm sign and estimated as:

$$\Delta E_n \simeq \gamma \lambda \left(\frac{\mu_B^3 H_z^3}{|n| m v^2} \right)^{\frac{1}{2}} \simeq 2 \cdot 10^{-3} \frac{\gamma \lambda}{|n|^{1/2}} H_z [\text{T}]^{3/2} \text{ K}, \quad (21)$$

$$\Delta E_0 \simeq 2 \gamma \mu_B H_z \simeq 1.3 \gamma H_z [\text{T}] \text{ K}. \quad (22)$$

Being very small for non-zero LLs, $n \neq 0$, this splitting should be observable for zero LL in high fields. Note that this effect has purely orbital origin and is completely decoupled from the additional Zeeman spin-splitting shown in Fig. 2d

$$\Delta E_s \simeq g \mu_B H \simeq 1.3 \frac{g}{2} H [\text{T}] \text{ K}, \quad g \approx 2, \quad (23)$$

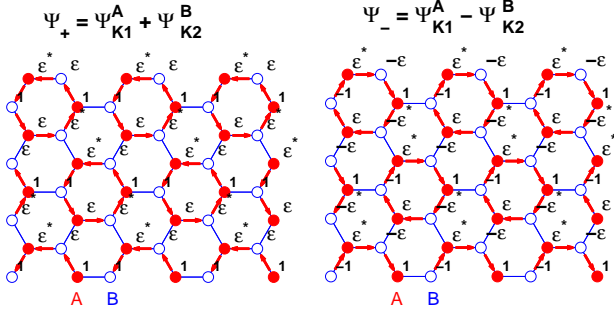


FIG. 3: Schematic of circular currents corresponding to Bloch functions $\Psi_{\pm} = \Psi_{K_1}^A \pm \Psi_{K_2}^B$ of the split zero Landau level.

because of very weak spin-orbital coupling. Unlike orbital-splitting, the spin-splitting is a function of the absolute value of \mathbf{H} (rather than of H_z), that permits separating the two contributions ΔE_s and ΔE_n by their angular field dependence.

To clarify the physical origin of the orbital splitting, consider the explicit form of the wave functions for carriers located on the up/down shifted zero LL:

$$\Phi_{\pm}^0(r) = \sum_{i=1}^4 F_{i\pm}^0(r) \Psi_i(r) = \Psi_{\pm}(r) f_0(r), \quad (24)$$

where the Bloch parts

$$\Psi_{\pm}(r) = \Psi_{K_1}^A(r) \pm \Psi_{K_2}^B(r), \quad (25)$$

are presented in Fig. 3 and can be interpreted as a set of clockwise and counterclock-wise current loops circulating around every third hexagon. Therefore, it is the orbital paramagnetic interaction of these *inter*-valley circular currents with H_z that causes the splitting ΔE_0 .

The current distribution for LLs with $n \neq 0$ is more complicated since both clockwise and counterclock-wise current loops with different envelope LL functions [$f_n(r)$ and $f_{n-1}(r)$] contribute to the wave functions of each split LL. The compensation of orbital momenta is almost complete, which explains the negligibly small splitting (21) of higher LLs. Note also that the additional contribution can be caused by the *intra*-valley circular currents circulating around next-nearest-neighbor plaquettes proposed in [18]. Governed by the next-nearest neighbor parameter λ , these currents do not contribute to $n = 0$ LL splitting and contribute only very weakly to the splitting of other LLs. Another consequence of the orbital LL splitting is the lattice period tripling produced by the network of circular current shown in Fig. 3. This field-induced breaking of graphene spatial symmetry can be observed for non-integer filling of zero LL, when clockwise and counterclock-wise currents do not compensate each other.

To conclude, we have proved that the orbital mechanism is sufficient to explain the zero LL splitting in

graphene. The effect occurs in a perturbative non-critical manner and is an intrinsic property of noninteracting fermions on a hexagonal lattice. As a consequence (observable optically), the orbital splitting should not depend on the LL filling factor, unlike the result from other models. At the same time, the many-body and/or disorder effects can amplify the orbital splitting (even for $n \neq 0$), induce an additional symmetry breaking, and bring about a nontrivial field and filling factor dependence of the gap observed experimentally [11, 12].

We are grateful to Y. Kopelevich and M. Dyakonov for valuable discussions. I.L. thanks the support of the ANR agency (project LoMaCoQuP).

-
- [1] I. A. Luk'yanchuk and Y. Kopelevich, Phys. Rev. Lett. **93**, 166402 (2004).
 - [2] K. S. Novoselov, A. K. Geim, S. V. Morozov *et al.*, Nature (London) **438**, 197 (2005).
 - [3] Y. Zhang, Y.-W. Tan, H. L. Stormer, and P. Kim, Nature (London) **438**, 201 (2005).
 - [4] S. Y. Zhou, G.-H. Gweon, J. Graf *et al.* Nature Phys. **2**, 595 (2006).
 - [5] A. Bostwick, T. Ohta, T. Seyller *et al.*, Nature Phys. **3**, 36 (2007).
 - [6] G. Li and E.Y. Andrei, Nature Phys., doi:10.1038/nphys653 (2007); arXiv:0705.1185.
 - [7] Y. Kopelevich, J.H.S. Torres, R.R. da Silva *et al.*, Phys. Rev. Lett. **90**, 156402 (2003).
 - [8] I. A. Luk'yanchuk and Y. Kopelevich, Phys. Rev. Lett. **97**, 256801 (2006).
 - [9] For a review see: M.I. Katsnelson and K.S. Novoselov, Solid St. Commun. **143**, 3 (2007).
 - [10] V. P. Gusynin and S. G. Sharapov, Phys. Rev. Lett. **95**, 146801 (2005).
 - [11] Y. Zhang, Z. Jiang, J. P. Small *et al.*, Phys. Rev. Lett. **96**, 136806 (2006).
 - [12] D. A. Abanin, K. S. Novoselov, U. Zeitler *et al.*, Phys. Rev. Lett. **98**, 196806 (2007).
 - [13] For a review see K. Yang, cond-mat/0703757.
 - [14] V. P. Gusynin, V. A. Miransky, and I. A. Shovkovy, Phys. Rev. Lett. **73**, 3499 (1994).
 - [15] H. A. Fertig and L. Brey, Phys. Rev. Lett. **97**, 116805 (2006).
 - [16] V. P. Gusynin, V. A. Miransky, S. G. Sharapov and I. A. Shovkovy, Phys. Rev. B **74**, 195429 (2006).
 - [17] D. V. Khveshchenko, Phys. Rev. Lett. **87**, 206401 (2001); *ibid.* **87**, 246802 (2001).
 - [18] J. Alicea and M. P. A. Fisher, Phys. Rev. B **74**, 075422 (2006).
 - [19] J.-N. Fuchs and P. Lederer, Phys. Rev. Lett. **98**, 016803 (2007).
 - [20] K. Nomura and A. H. MacDonald, Phys. Rev. Lett. **96**, 256602 (2006).
 - [21] M. O. Goerbig, R. Moessner, and B. Douçot, Phys. Rev. B **74**, 161407 (2006).
 - [22] D. A. Abanin, P. A. Lee, and L. S. Levitov, Phys. Rev. Lett. **98**, 156801 (2007).
 - [23] A. H. Castro Neto, F. Guinea, and N. M. R. Peres, Phys. Rev. B **73**, 205408 (2006).

- [24] D. A. Abanin, P. A. Lee, and L. S. Levitov, Phys. Rev. Lett. **96**, 176803 (2006).
- [25] L. D. Landau and E. M. Lifshitz, *Statistical Physics*, Part 1 (Butterworth-Heinemann, Oxford, 1980).
- [26] O.V. Kovalev, *Presentation of Crystallographic Space Groups: Irreducible Representations, Induced Representations, and Corepresentations* (CRC Press, 1993).
- [27] E. McCann, K. Kechedzhi, V. I. Fal'ko *et al.*, Phys. Rev. Lett. **97**, 146805 (2006).
- [28] E. M. Lifshitz and L. P. Pitaevskii, *Statistical Physics*, Part 2 (Butterworth-Heinemann, Oxford, 2002).
- [29] E. I. Blount, Phys. Rev. **126**, 1636 (1962).
- [30] J. L. Mañes, F. Guinea, and M. A. H. Vozmediano, Phys. Rev. B **75**, 155424 (2007).